frontiers in Communications and Networks

ORIGINAL RESEARCH
published: 20 October 2021
doi: 10.3389/frcmn.2021.734165

Optimal Signaling Schemes and Sum-Capacity of 1-bit ADC Fading 2-User MACs under Gaussian-Mixture Interference

Md Hasan Rahman[1], *Mohammad Ranjbar*[1], *Nghi H. Tran*[1]* *and Khanh Pham*[2]

[1]Department of Electrical and Computer Engineering, University of Akron, Akron, OH, United States, [2]Air Force Research Laboratory, Kirtland Air Force Base, Albuquerque, NM, United States

In this work, we establish the sum-capacity-achieving signaling schemes and the sum-capacity of a 2-user multiple access Rayleigh fading channel with 1-bit output quantization in the presence of Gaussian-mixture co-channel interference. The considered Gaussian mixture channel is an accurate model to capture non-Gaussian co-channel interference plus noise in practical wireless networks under coexistence regimes, especially for those having heterogeneous structures and high frequency reuse factor. By first examining the phases of the optimal input signals, we demonstrate that these phases must be $\pi/2$ circularly symmetric. As a result, the problem of optimizing the sum-rate is equivalent to minimizing the conditional output entropy. By establishing the Kuhn-Tucker condition on the optimal amplitude input distributions, we then show that the optimal input amplitudes are bounded. Our proof relies on the convexity of the log of sum of Q functions. Then, given the linearity of the conditional entropy over the feasible set of bounded amplitude distributions, it is concluded that the optimal input signals must have constant amplitudes. Therefore, the use of any $\pi/2$ circularly symmetric signaling schemes with constant amplitudes and full power are sum-capacity-achieving. Using these optimal input signals, the sum-capacity can finally be calculated.

Keywords: 1-bit ADC, achievable rate, Gaussian-mixture interference, multiple access channel, rayleigh fading, sum-capacity

OPEN ACCESS

Edited by:
Ebrahim Bedeer, University of Saskatchewan, Canada

Reviewed by:
Lukas T. N. Landau, Pontifical Catholic University of Rio de Janeiro, Brazil
Chinmoy Kundu, University College Dublin, Ireland

***Correspondence:**
Nghi H. Tran
nghi.tran@uakron.edu

Specialty section:
This article was submitted to Communications Theory, a section of the journal Frontiers in Communications and Networks

Received: *30 June 2021*
Accepted: *16 September 2021*
Published: *20 October 2021*

Citation:
Rahman MH, Ranjbar M, Tran NH and Pham K (2021) Optimal Signaling Schemes and Sum-Capacity of 1-bit ADC Fading 2-User MACs under Gaussian-Mixture Interference. Front. Comms. Net 2:734165. doi: 10.3389/frcmn.2021.734165

1 INTRODUCTION

Given the significant benefit in power and cost saving of 1-bit analog-digital-converter (ADC), considerable efforts have been dedicated to signal designs and processing techniques for this ultra-low resolution ADC in high-bandwidth and/or multi-antenna systems Liu et al. (2019); Jeon et al. (2019); Choi et al. (2020); Xu et al. (2018); Zhang et al. (2016); Mo et al. (2017); Mollen et al. (2017); Xiong et al. (2017); Jacobsson et al. (2017); Studer and Durisi (2016). Over the years, several interesting information-theoretical results have been obtained for both point-to-point and multi-user channels with 1-bit ADC under additive white Gaussian noise (AWGN). For example, it has been shown in Singh et al. (2009); Mo and Heath (2015) that Quadrature phase Shift Keying (QPSK) is capacity-achieving in point-to-point single- and multiple-antenna static channels. Optimal signaling schemes and fundamental limits of 1-bit ADC have also been established for

point-to-point fading channels in Krone and Fettweis (2010); Mezghani and Nossek (2008); Vu et al. (2018), Vu et al. (2019). Recently, under the assumption of AWGN, signal design and fundamental limits of 1-bit ADC have also been extended to multi-user static channels Rassouli et al. (2018) and multi-user fading channels (Ranjbar et al., 2019; Ranjbar et al., 2020). Specifically, it was shown in Rassouli et al. (2018) that any point in the capacity region of a 2-user static Gaussian multiple access channel (MAC) can be achieved by input signals with bounded supports. Furthermore, an upper bound on the sum-capacity was also developed in Rassouli et al. (2018). However, to our knowledege, the detailed characteristics of the optimal signals for such static Gaussian MACs remain unknown. In Ranjbar et al. (2020), by exploiting the effect of fading, the detailed characteristics of optimal input signals on the boundary of the capacity region of a 2-user Gaussian fading MAC with 1-bit ADC were also addressed.

Current and future active wireless systems (AWSs) such as 5G and beyond cellular networks with their multi-tier heterogeneous architectures are being designed to operate in the same or adjacent spectrum to other existing wireless systems. For example, proliferation in the number of wireless users and devices fueled by emerging applications in e.g., Internet of Things (IoT), unmanned systems, wearable technology, remote sensing is leading to the design of active-active coexistence such as LTE-U and WiFi in unlicensed bands, and incumbent, priority and general authorized access in Citizens Broadband Radio Service (CBRS) bands FCC (2020). Such coexistence is intensifying concerns on co-channel and adjacent-channel interference and its management for wireless systems. Specifically, AWSs themselves need to cope with increased active co-channel interference, which is generated in different ways. For example, due to their heterogeneous structures and the high frequency reuse factor, future AWSs require sharing of time-frequency resources with existing users and this makes intercell interference no longer negligible Osseiran et al. (2014); Chen and Zhao (2014); Feng et al. (2014); Lin et al. (2014); Fodor et al. (2012). In addition, radio frequency interference (RFI) mitigation might not be perfect, which leads to residual interference. Such intermittence and asynchronism make the statistical properties of RFI at AWS complicated. In particular, the traditional approach of treating co-channel interference plus noise as Gaussian no longer holds Irio et al., 2020; Irio et al., 2019; ElSawy et al. (2013); Lin et al. (2014). For example, aggregate interference generated by small cells to macro cells are non-Gaussian. It is due to the effect of dominant interferers, and the central limit theorem no longer holds Quek et al. (2013). In many wireless networks, especially heterogeneous AWSs, co-channel interference plus noise can be accurately modeled as Gaussian mixture (GM) Irio et al. (2020); Quek et al. (2013); Gulati et al. (2010); Stein (1995); Middleton (1999); Wang and Poor (1999); MIT Lincoln Laboratory (Reynolds, 2009); Erseghe et al. (2008); Moghimi et al. (2011); Bayram and Gezici (2010); Nasri and Schober (2009); Kenarsari-Anhari and Lampe (2010); Bhatia and Mulgrew (2007).

During the last few years, there have been several contributions on fundamental limits and optimal signal designs for non-Gaussian AWSs Das (2000); Fahs et al. (2012); Tchamkerten (2004); Oettli (1974); Cao et al. (2014); Vu et al. (2015); Ranjbar et al. (2018); Dytso et al. (2017). However, the results are rather limited. It is because for non-Gaussian channels, the assumption of having Gaussian input signals is no longer valid. Due to the difficulty in studying the detailed properties of the optimal inputs and in establishing the capacity in closed-form for a non-Gaussian channel, numerical methods are usually need to find the capacity-achieving signal, even for a point-to-point channel Vu et al. (2015); Le et al. (2016). In our recent work in Rahman et al. (2020a), Rahman et al. (2020b), the detailed characteristics of a capacity-achieving scheme were studied for a point-to-point Gaussian mixture channel using 1-bit output quantization. In particular, it was shown in Rahman M. H. et al. (2020) that for a general GM channel, the maximum number of mass points in the optimal signal is four. In addition, under the special case of zero-mean GM components, QPSK is optimal. Unfortunately, at the network level, signal design and network information-theoretical results for non-Gaussian noise and interference are complete lacking. Therefore, considering non-Gaussian interference plus noise in multi-user AWSs presents new challenges.

Motivated by the above discussions, we investigate the network information-theoretical limits of a 2-user multiple access Rayleigh fading channel with 1-bit output quantization in the presence of Gaussian-mixture co-channel interference. Specifically, we establish the sum-capacity-achieving signaling schemes and the sum-capacity of the considered GM MAC, which is an accurate model to capture non-Gaussian co-channel interference plus noise in practical wireless networks under coexistence regimes, especially for those having heterogeneous structures and high frequency reuse factor. In general, the problem of maximizing the sum-rate over input signals to determine the sum-capacity is both analytically and computationally challenging, especially on the space of multi-dimensional probability distributions with a non-linear mapping from the inputs to the output and non-Gaussian noise plus interference. Therefore, the main contribution of this work lies in the explicit establishment of optimal signaling schemes for such non-linear and non-Gaussian multi-user channels. Our approach is to separate the phases and amplitudes of the input signals to study their effects to the main sum-rate optimization problem. The specific contributions of our work can be summarized as follows:

- In the first part of our work, we demonstrate that the phases of the optimal inputs must be $\pi/2$ circularly symmetric. While this property has been shown before over various 1-bit ADC single-user, it is not trivial to extend to multi-user channels in the presence GM noise. Given the $\pi/2$ circularly symmetric property, it is then demonstrated that the problem of optimizing the sum-rate is equivalent to minimizing the conditional output entropy.
- More importantly, in the second part of the paper, by establishing and examining the Kuhn-Tucker condition

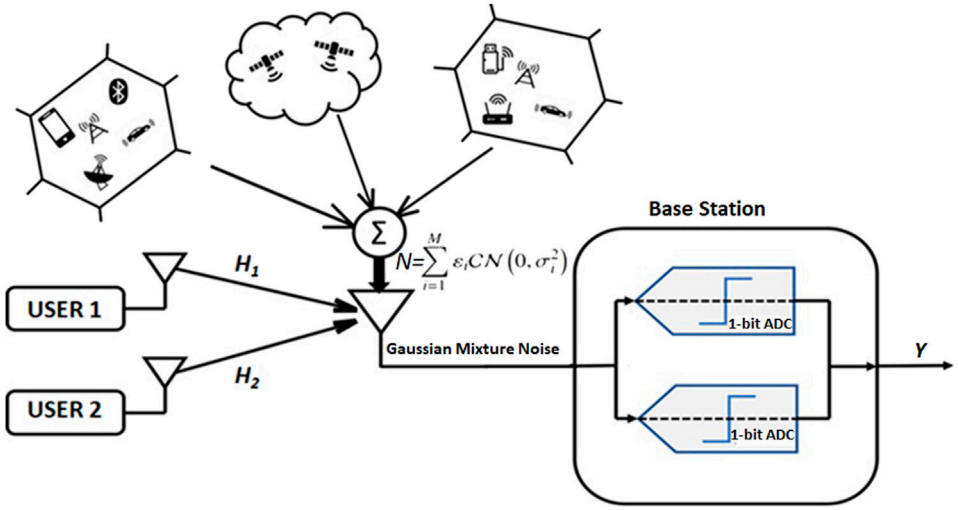

FIGURE 1 | A 2-user fading MAC under GM noise plus interference with 1-bit output quantization.

(KTC) on the optimal amplitude input distributions, we then show that the optimal input amplitudes are bounded. Towards this end, we exploit the convexity of the log of sum of Q functions to deal with the presence of a mixture of Gaussian components. Furthermore, since the main objective function is now linear over the feasible set of bounded amplitude distributions, it achieves the minimum value at an extreme point. As a result, we can conclude that the optimal input signals must have constant amplitudes. Therefore, the use of any $\pi/2$ circularly symmetric signaling schemes with constant amplitudes and full power are sum-capacity-achieving. Using these optimal input signals, the sum-capacity can finally be established

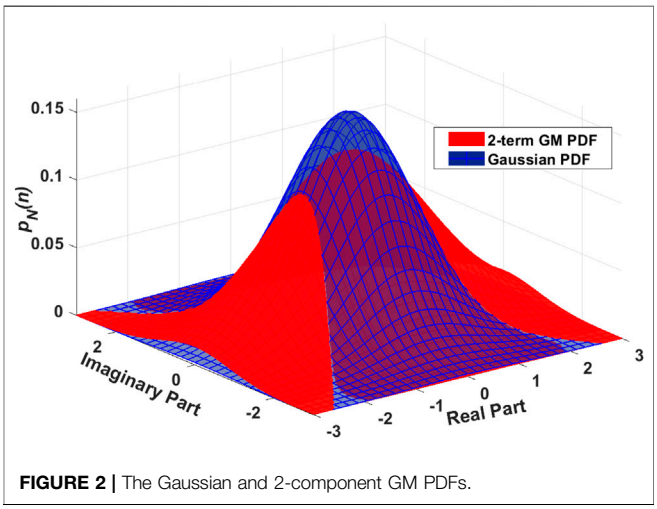

FIGURE 2 | The Gaussian and 2-component GM PDFs.

2 A 2-USER MAC IN RAYLEIGH FADING WITH 1-BIT ADC AND ACHIEVABLE SUM-RATE

2.1 Channel Model

We consider a 2-user multiple access channel (MAC) under GM noise plus interference N as depicted in **Figure 1**. The two users transmit their own signals X_1 and X_2, respectively, to the base station being equipped with an 1-bit ADC. These two transmitted signals X_1 and X_2 are imposed by the power constraints $E\left[|X_1|^2\right] \le P_1$ and $E\left[|X_2|^2\right] \le P_2$. The complex signal Z received at the base station is given as

$$Z = H_1X_1 + H_2X_2 + N. \tag{1}$$

Here, the total noise plus interference N follows a GM distribution, which is a mixture of M Gaussian components, and its probability density function (PDF) is given as

$$p_N(n) = \sum_{i=1}^{M} \varepsilon_i \mathcal{CN}(n, 0, \sigma_i^2). \tag{2}$$

In **Eq. 2**, $\mathcal{CN}(n, 0, \sigma_i^2)$, $1 \le i \le M$, is the ith complex Gaussian component with mean zero and variance σ_i^2, and $\{\varepsilon_i\}$ are the mixing probabilities satisfying $\sum_{i=1}^{M}\varepsilon_i = 1$. Note that for a given complex realization n of N, $p_N(n)$ in **Eq. 2** gives us the value of the PDF at that complex point n. As an illustrative example, **Figure 2** shows the traditional Gaussian PDF and the 2-term GM PDF, both having zero mean and unit variance. Note that for the 2-term GM PDF, we use $\varepsilon_1 = 0.2$, $\varepsilon_2 = 0.8$, $\sigma_1^2 = 2$, and $\sigma_2^2 = 0.75$.

Furthermore, in **Eq. 1**, H_1 and H_2 are the complex fading gains from user 1 and user 2 to the base station, respectively. In this paper, we consider Rayleigh fading channels, where H_1 and H_2 are circular symmetric Gaussian random variables with mean zero and variance γ_1^2 and γ_2^2. Their PDFs are given as

$$\begin{aligned} f_{H_1}(h_1) &= \mathcal{CN}(h_1, 0, \gamma_1^2), \\ f_{H_2}(h_2) &= \mathcal{CN}(h_2, 0, \gamma_2^2). \end{aligned} \tag{3}$$

In addition, the fading channel gains are assumed to be known at the base station, but not the users, and they change independently over time.

With 1-bit output quantization, the real and imaginary parts of the received signal Z will be fed through a 1-bit quantizer, which results in the following complex binary outputs:

$$Y = Quant(Z) = Quant(H_1X_1 + H_2X_2 + N), \tag{4}$$

where $Quant(\cdot)$ is the 1-bit quantization operation defined as:

$$Quant(x) = \begin{cases} 1 & x \geq 0 \\ -1 & x < 0. \end{cases} \tag{5}$$

It is then easy to see that the output Y can only take on one of the following values in $\mathcal{Y} = \{1+1j, 1-1j, -1+1j, -1-1j\}$.

2.2 Ergodic Sum-Rate and Sum-Capacity

For a given set of input distributions $F_{X_1}(x_1)$ and $F_{X_2}(x_2)$, the ergodic sum-rate of the considered MAC is the joint mutual information (MI) between the inputs X_1 and X_2 and the output Y, which is given as Gamal and Kim (2011).

$$I(X_1, X_2; Y \mid H_1, H_2) = E_{H_1,H_2}[I(X_1, X_2; Y \mid H_1 = h_1, H_2 = h_2)]. \tag{6}$$

In **Eq. 6**, the expectation $E[\cdot]$ is performed over fading gains H_1 and H_2, and $I(X_1, X_2; Y \mid H_1 = h_1, H_2 = h_2)$ is the conditional joint MI for given $H_1 = h_1$ and $H_2 = h_2$. The ergodic sum-rate can be expressed in terms of joint and output entropies as follows:

$$\begin{aligned} I(X_1, X_2; Y \mid H_1, H_2) &= H(Y; F_{X_1}, F_{X_2} \mid H_1, H_2) \\ &\quad - H(Y \mid X_1, X_2, H_1, H_2). \end{aligned} \tag{7}$$

In **Eq. 7**, the joint entropy $H(Y; F_{X_1}, F_{X_2} \mid H_1, H_2)$ is calculated as

$$\begin{aligned} &H(Y; F_{X_1}, F_{X_2} \mid H_1, H_2) = E_{H_1,H_2}[H(Y; F_{X_1}, F_{X_2} \mid H_1 = h_1, H_2 = h_2)] \\ &= -\int_{H_1}\int_{H_2} \sum_{y\in Y} p(y; F_{X_1}, F_{X_2} | H_1 = h_1, H_2 = h_2) \\ &\times \log p(y; F_{X_1}, F_{X_2} | H_1 = h_1, H_2 = h_2) dF_{H_1} dF_{H_2}. \end{aligned} \tag{8}$$

Note that F_{H_1} and F_{H_2} are the cumulative distribution functions (CDFs) of H_1 and H_2, respectively, and $dF_{H_1} = f_{H_1}dh_1$ and $dF_{H_2} = f_{H_2}dh_2$, where the PDFs f_{H_1} and f_{H_2} are given in **Eq. 3**. In addition, $p(y; F_{X_1}, F_{X_2} | H_1 = h_1, H_2 = h_2)$ is the joint density function for given fading realizations $H_1 = h_1$ and $H_2 = h_2$, which can be calculated as

$$\begin{aligned} &p(y; F_{X_1}, F_{X_2} | H_1 = h_1, H_2 = h_2) \\ &= \int_{x_1}\int_{x_2} p(y | X_1 = x_1, X_1 = x_1, H_1 = h_1, H_2 = h_2) dF_{X_1} dF_{X_2}, \end{aligned} \tag{9}$$

where

$$\begin{aligned} &p(y | X_1 = x_1, X_1 = x_1, H_1 = h_1, H_2 = h_2) \\ &= \sum_{i=1}^{M} \varepsilon_i Q\left(-\frac{\sqrt{2}\,\Re(x_1h_1 + x_2h_2)\Re(y)}{\sigma_i}\right) Q\left(-\frac{\sqrt{2}\,\Im(x_1h_1 + x_2h_2)\Im(y)}{\sigma_i}\right). \end{aligned} \tag{10}$$

It should be mentioned that $y \in \mathcal{Y}$. Furthermore, in **Eq. 10**, $Q(x) = \frac{1}{\sqrt{2\pi}}\int_x^\infty e^{-\frac{v^2}{2}} dv$ is the well-known Q function, and $\Re(\cdot)$ and $\Im(\cdot)$ represent the real and imaginary parts of a complex number, respectively. In addition, the conditional output entropy can be written as:

$$\begin{aligned} &H(Y \mid X_1, X_2, H_1, H_2) = E_{H_1,H_2}[H(Y \mid X_1, X_2, H_1 = h_1, H_2 = h_2)] \\ &= -\int_{H_1}\int_{H_1}\int_{X_1}\int_{X_2} \sum_{y\in Y} p(y | X_1 = x_1, X_2 = x_1, H_1 = h_1, H_2 = h_2) \\ &\times \log p(y | X_1 = x_1, X_2 = x_2, H_1 = h_1, H_2 = h_2) dF_{X_1} dF_{X_2} dF_{H_1} dF_{H_2}. \end{aligned} \tag{11}$$

For simplicity, hereafter, we shall use the notations $p(y|x_1, x_2, h_1, h_2)$ and $p(y; F_{X_1}, F_{X_2} \mid h_1, h_2)$ to refer to the density functions $p(y|X_1 = x_1, X_2 = x_2, H_1 = h_1, H_2 = h_2)$ and $p(y; F_{X_1}, F_{X_2} \mid H_1 = h_1, H_2 = h_2)$, respectively.

The ergodic sum-capacity C_s of the considered MAC is the maximum ergodic sum-rate over all feasible input distributions $F_{X_1}(x_1)$ and $F_{X_2}(x_2)$ under the power constraints, which is given as:

$$C_s = \max_{\substack{F_{X_1}, F_{X_2} \\ E\left[|X_j|^2\right] \leq P_j, j=1,2}} I(X_1, X_2; Y \mid H_1, H_2). \tag{12}$$

3 SUM-CAPACITY ACHIEVING INPUT SIGNALS

In general, the problem of maximizing MI over input distributions under certain input constraints as in **Eq. 12** has been extensively studied, but tractable solutions can only be obtained for very few specific cases when the mapping from the inputs to output is linear, and the noise is additive Gaussian. Unfortunately, for the considered non-Gaussian channel, we have a non-linear mapping from the inputs to the output under the presence of GM noise. Therefore, this optimization problem is not trivial. In the following, our approach to solve **Eq. 12** is to first address the optimal phases. The optimal amplitude distributions are then investigated to determine the complete input distributions.

3.1 Optimal Phase Distributions

To examine the effect of the input phase distributions, we first re-write the conditional density function in **Eq. 10** using the amplitudes and phases as:

$$\begin{aligned} &p(y \mid x_1, x_2, h_1, h_2) \\ &= \sum_{i=1}^{M} \varepsilon_i Q\left(-\frac{\sqrt{2}\,(|h_1||x_1|\cos(\theta_{x_1} + \theta_{h_1}) + |h_2||x_2|\cos(\theta_{x_2} + \theta_{h_2}))}{\sigma_i} \Re(y)\right) \\ &\times Q\left(-\frac{\sqrt{2}\,(|h_1||x_1|\sin(\theta_{x_1} + \theta_{h_1}) + |h_2||x_2|\sin(\theta_{x_2} + \theta_{h_2}))}{\sigma_i} \Im(y)\right). \end{aligned} \tag{13}$$

The joint and output entropies in **Eqs. 8, 11**, respectively, can then be expressed as

$$
\begin{aligned}
&H(Y;F_{X_1},F_{X_2}\mid H_1,H_2)=E_{H_1,H_2}\left[H(Y;F_{X_1},F_{X_2}\mid H_1=h_1,H_2=h_2)\right]\\
&=\int_{H_1}\int_{H_2}\sum_{y\in Y}\left[\left\{\int_{X_1}\int_{X_2}\sum_{i=1}^{M}\varepsilon_i Q\left(-\frac{\sqrt{2}\left(|h_1\|x_1|\cos(\theta_{x_1}+\theta_{h_1})+|h_2\|x_2|\cos(\theta_{x_2}+\theta_{h_2})\right)}{\sigma_i}\Re(y)\right)\right.\right.\\
&\times Q\left.\left(-\frac{\sqrt{2}\left(|h_1\|x_1|\sin(\theta_{x_1}+\theta_{h_1})+|h_2\|x_2|\sin(\theta_{x_2}+\theta_{h_2})\right)}{\sigma_i}\Im(y)\right)dF_{X_1}dF_{X_2}\right\}\\
&\times\log\left\{\int_{X_1}\int_{X_2}\sum_{i=1}^{M}\varepsilon_i Q\left(-\frac{\sqrt{2}\left(|h_1\|x_1|\cos(\theta_{x_1}+\theta_{h_1})+|h_2\|x_2|\cos(\theta_{x_2}+\theta_{h_2})\right)}{\sigma_i}\Re(y)\right)\right.\\
&\times Q\left.\left.\left(-\frac{\sqrt{2}\left(|h_1\|x_1|\sin(\theta_{x_1}+\theta_{h_1})+|h_2\|x_2|\sin(\theta_{x_2}+\theta_{h_2})\right)}{\sigma_i}\Im(y)\right)dF_{X_1}dF_{X_2}\right\}\right]dF_{H_1}dF_{H_2},
\end{aligned}
\tag{14}
$$

and

$$
\begin{aligned}
&\mathbf{H}(Y|F_{X_1},F_{X_2},H_1,H_2)\\
&=\int_{H_1}\int_{H_2}\int_{X_1}\int_{X_2}\xi\left\{\sum_{i=1}^{M}\varepsilon_i Q\left(-\frac{\sqrt{2}\left(|h_1\|x_1|\cos(\theta_{x_1}+\theta_{h_1})+|h_2\|x_2|\cos(\theta_{x_2}+\theta_{h_2})\right)}{\sigma_i}\Re(y)\right)\right.\\
&\times\left.Q\left(-\frac{\sqrt{2}\left(|h_1\|x_1|\sin(\theta_{x_1}+\theta_{h_1})+|h_2\|x_2|\sin(\theta_{x_2}+\theta_{h_2})\right)}{\sigma_i}\Im(y)\right)\right\}dF_{X_1}dF_{X_2}dF_{H_1}dF_{H_2}\Big].
\end{aligned}
\tag{15}
$$

In **Eq. 15**, $\xi(\cdot)$ is an entropy function of the distribution in **Eq. 10**, which is calculated as:

$$
\begin{aligned}
&\xi\left\{\sum_{i=1}^{M}\varepsilon_i Q(f_R(x_1,x_2,h_1,h_2)\Re(y))Q(f_I(x_1,x_2,h_1,h_2)\Im(y))\right\}\\
&=-\sum_{y\in Y}\left(\sum_{i=1}^{M}\varepsilon_i Q(f_R(x_1,x_2,h_1,h_2)\Re(y))Q(f_I(x_1,x_2,h_1,h_2)\Im(y))\right)\\
&\times\log\left(\sum_{i=1}^{M}\varepsilon_i Q(f_R(x_1,x_2,h_1,h_2)\Re(y))Q(f_I(x_1,x_2,h_1,h_2)\Im(y))\right).
\end{aligned}
\tag{16}
$$

To determine the optimal phases of the input signals, for a given set of the inputs F_{X_1} and F_{X_2}, construct the following two other input distributions:

$$
\begin{aligned}
F_{X_1}^{\pi/2}(x_1)&=\frac{1}{4}\sum_{k=0}^{3}F_{X_1}\left(x_1e^{j\frac{k\pi}{2}}\right),\\
F_{X_2}^{\pi/2}(x_2)&=\frac{1}{4}\sum_{l=0}^{3}F_{X_2}\left(x_2e^{j\frac{l\pi}{2}}\right).
\end{aligned}
\tag{17}
$$

It is not difficult to verify that the two new distributions are $\pi/2$ circularly symmetric. Note that a density function $F_X(X)$ is $\pi/2$ circularly symmetric if $F_X(X)=F_X\left(Xe^{j\pi/2}\right)$ for any integer j. As we demonstrate in **Appendix A**, the use of $F_{X_1}^{\pi/2}(x_1)$ and $F_{X_2}^{\pi/2}(x_2)$ results in a uniform output Y, and the corresponding output entropy in **Eqs. 8, 14** will be maximized, and it is equal to 2. Now, let compare the conditional entropy in **Eq. 15** for two pairs of inputs, $\left(F_{X_1(x_1)},F_{X_2(x_2)}\right)$ and $\left(F_{X_1}^{\pi/2}(x_1),F_{X_2}^{\pi/2}(x_2)\right)$. We first write this conditional entropy when the pair $\left(F_{X_1}^{\pi/2}(x_1),F_{X_2}^{\pi/2}(x_2)\right)$ is used as:

$$
\begin{aligned}
&\mathbf{H}\left(Y|F_{X_1}^{\pi/2},F_{X_2}^{\pi/2},H_1,H_2\right)\\
&=\int_{H_1}\int_{H_2}\int_{X_2}\int_{X_1}\frac{1}{16}\sum_{k=0}^{3}\sum_{l=0}^{3}\xi\left\{\sum_{i=1}^{M}\varepsilon_i Q\left(-\frac{\sqrt{2}\left(|h_1\|x_1|\cos(\theta_{x_1}+\theta_{h_1})+|h_2\|x_2|\cos(\theta_{x_2}+\theta_{h_2})\right)}{\sigma_i}\Re(y)\right)\right.\\
&\times\left.Q\left(-\frac{\sqrt{2}\left(|h_1\|x_1|\sin(\theta_{x_1}+\theta_{h_1})+|h_2\|x_2|\sin(\theta_{x_2}+\theta_{h_2})\right)}{\sigma_i}\Im(y)\right)\right\}dF_{X_1}\left(x_1e^{j\frac{k\pi}{2}}\right)dF_{X_2}\\
&\left(x_2e^{j\frac{l\pi}{2}}\right)dF_{H_1}dF_{H_2}
\end{aligned}
\tag{18}
$$

Because we consider Rayleigh fading, and the channel is ergodic, the expectation over H_1 and H_2 in **Eq. 18** can be written in terms of their amplitudes and phases as $E_{H_1}E_{H_2}=E_{|H_1|}E_{|H_2|}E_{\theta_{H_1}}E_{\theta_{H_2}}$. Furthermore, we know that the phases of fading gains $(\theta_{H_1},\theta_{H_2})$ are uniform. As such, the inner expectations over $(\theta_{H_1},\theta_{H_2})$ do not depend on the phases of the inputs (ϕ_{X_1},ϕ_{X_2}). Following the same argument as in Ranjbar et al. (2020), we can simply let $\phi_{X_1}=\phi_{X_2}=0$ without changing the conditional entropy. Therefore, we have:

$$
\begin{aligned}
&\mathbf{H}\left(Y|F_{X_1}^{\pi/2},F_{X_2}^{\pi/2},H_1,H_2\right)\\
&=\int_{H_1}\int_{H_2}\int_{|X_2|}\int_{|X_1|}\frac{1}{16}\sum_{k=0}^{3}\sum_{l=0}^{3}\xi\left\{\sum_{i=1}^{M}\varepsilon_i Q\left(-\frac{\sqrt{2}\left(|h_1\|x_1|\cos(\theta_{h_1})+|h_2\|x_2|\cos(\theta_{h_2})\right)}{\sigma_i}\Re(y)\right)\right.\\
&\times\left.Q\left(-\frac{\sqrt{2}\left(|h_1\|x_1|\sin(\theta_{h_1})+|h_2\|x_2|\sin(\theta_{h_2})\right)}{\sigma_i}\Im(y)\right)\right\}dF_{X_1}\left(x_1e^{j\frac{k\pi}{2}}\right)dF_{X_2}\\
&\left(x_2e^{j\frac{l\pi}{2}}\right)dF_{H_1}dF_{H_2}\\
&=\int_{H_1}\int_{H_2}\int_{|X_2|}\int_{|X_1|}\xi\left\{\sum_{i=1}^{M}\varepsilon_i Q\left(-\frac{\sqrt{2}\left(|h_1\|x_1|\cos(\theta_{h_1})+|h_2\|x_2|\cos(\theta_{h_2})\right)}{\sigma_i}\Re(y)\right)\right.\\
&\times\left.Q\left(-\frac{\sqrt{2}\left(|h_1\|x_1|\sin(\theta_{h_1})+|h_2\|x_2|\sin(\theta_{h_2})\right)}{\sigma_i}\Im(y)\right)\right\}dF_{X_1}(x_1)dF_{X_2}(x_2)dF_{H_1}dF_{H_2}\\
&=\mathbf{H}(Y|X_1,X_2,H).
\end{aligned}
\tag{19}
$$

Since the two conditional entropies are the same, it is then clear that the use of $(F_{X_1}^{\pi/2},F_{X_2}^{\pi/2})$ leads to a better sum-rate. As a result, it can be concluded that the optimal input distributions are $\pi/2$ circularly symmetric. With such input signals, the output entropy in **Eq. 8** is 2. Therefore, from **Eq. 7**, the sum-rate maximization problem to find the sum-capacity C_s in **Eq. 12** becomes a minimization problem of the conditional output entropy as:

$$
C_s=2-\min_{\substack{F_{X_1},F_{X_2}\\ E\left[|X_j|^2\right]\le P_j,j=1,2}}\mathbf{H}(Y|X_1,X_2,H_1,H_2),
\tag{20}
$$

where F_{X_1} and F_{X_2} are both $\pi/2$ circularly symmetric. Since the objective function $\mathbf{H}(Y|X_1,X_2,H_1,H_2)$ is the function of F_{X_1} and F_{X_2} only, for the sake of convenience, we will use $\mathbf{H}(F_{X_1},F_{X_2})$ to refer to $\mathbf{H}(Y|X_1,X_2,H_1,H_2)$. The optimal solutions, denoted as $F_{X_1}^{**}$ and $F_{X_1}^{**}$, can be therefore expressed as:

$$
\left(F_{X_1}^{**},F_{X_2}^{**}\right)=\arg\min_{E\left[|X_1|^2\right]\le P_1,E\left[|X_2|^2\right]\le P_2}\mathbf{H}\left(F_{X_1},F_{X_2}\right).
\tag{21}
$$

3.2 Optimal Amplitude Distributions

Given the characteristic of the optimal phases established in the previous section, we now turn out attention to the optimality of the amplitude distributions.

To provide more insights on the solutions of **Eq. 21**, we first examine a simplified optimization problem by fixing the distribution F_{X_2}. In particular, we know that the set of input probability distributions with second moment constraint is convex and compact Abou-Faycal et al. (2001). Furthermore, $\mathbf{H}(F_{X_1},F_{X_2})$ is a continuous function of F_{X_1} Ranjbar et al. (2020). Therefore, if we select a fixed distribution F_{X_2}, there always exists an optimal solution $F_{X_1}^{*}$ to minimize $\mathbf{H}(F_{X_1},F_{X_2})$. That is:

$$
F_{X_1}^{*}=\arg\min_{F_{X_1},E\left[|X_1|^2\right]\le P_1}\mathbf{H}\left(F_{X_1},F_{X_2}\right).
\tag{22}
$$

We know that the entropy function $\mathbf{H}(F_{X_1},F_{X_2})$ is weak continuous and weakly differentiable of F_{X_1} Borwein and Lewis (2010). Therefore, we can establish the Kuhn-Tucker condition (KTC) for which a distribution $F_{X_1}^{*}$ is the solution of **Eq. 22** as follows:

$$D_{F^*_{X_1}}\left(\mathbf{H}(F_{X_1},F_{X_2}),F_{X_1}-F^*_{X_1}\right) + \mu_1 D_{F^*_{X_1}}\left(g(F_{X_1}),F_{X_1}-F^*_{X_1}\right)\geq 0 \quad \forall F_{X_1}, \tag{23}$$

where μ_1 is the Lagrangian multiplier and D (·) is the directional derivative. Before examining further the above KTC, we state the following result regarding μ_1.

Proposition 1. The Lagrangian multiplier μ_1 in **Eq. 23** is positive. Equivalently, for the optimization problem in **Eq. 22**, full-power P_1 is used.

Proof. Let Ω_1 is the set of the feasible set of F_{X_1} that satisfies $E[|X_1|^2] \leq P_1$. The first consequence of having $\pi/2$ circularly symmetric input is that for a fixed F_{X_2}, $\mathbf{H}(F_{X_1},F_{X_2})$ is a linear function of F_{X_1} and power constraint $g(F_{X_1}) = \int |x_1|^2 dF_{X_1} - P_1$ is a linear function of F_{X_1} Cover and Thomas (2006). It is then clear that the objective function $\mathbf{H}(F_{X_1},F_{X_2})$ achieves its minimum an extreme point of Ω_1 Winkler (1988). In the following, we will show that any distribution with the second moment being smaller than P_1 is not an extreme point of the set. Towards this end, let consider a distribution F_{X_t} on Ω_1 such that $E[|X_t|^2] = P_t < P_1$. Let us assume, there exists a positive δ such that $0 < P_t - \delta$, $P_t + \delta < P_1$. In addition, we define, $F_{X'_t} = \sqrt{\frac{P_t-\delta}{P_t}}F_{X_t}$ and $F_{X''_t} = \sqrt{\frac{P_t+\delta}{P_t}}F_{X_t}$. It is obvious that $E\left[|X'_t|^2\right] = \frac{P_t-\delta}{P_t}E\left[|X'_t|^2\right] = P_t - \delta$ and $E\left[|X''_t|^2\right] = P_t + \delta$. Which means both $F_{X'_t}$ and $F_{X''_t}$ are in Ω_1. Now, consider the following linear combination:

$$\begin{aligned} tF_{X'_t} + (1-t)F_{X''_t} &= \left(t\sqrt{\frac{P_t-\delta}{P_t}} + (1-t)\sqrt{\frac{P_t+\delta}{P_t}}\right)F_{X_t} \\ &= \left(t\left(\sqrt{\frac{P_t-\delta}{P_t}} - \sqrt{\frac{P_t+\delta}{P_t}}\right) + \sqrt{\frac{P_t+\delta}{P_t}}\right)F_{X_t}. \end{aligned} \tag{24}$$

It can then be verified that when choosing t such as:

$$t = \frac{\sqrt{\frac{P_t+\delta}{P_t}} - 1}{\sqrt{\frac{P_t+\delta}{P_t}} - \sqrt{\frac{P_t-\delta}{P_t}}},$$

we have $tF_{X'_t} + (1-t)F_{X''_t} = F_{X_t}$. Thus, F_{X_t} is a convex combination of two other distributions in the feasible set. Therefore, F_{X_t} cannot be an extreme point on the set Ω_1 Winkler (1988). It can then be concluded that the power constraint must be active, and μ_1 is positive.

With a positive μ_1, we shall analyze the properties of the amplitude of $F^*_{X_1}$. To do that, we re-write the entropy $\mathbf{H}(F_{X_1},F_{X_2})$ as:

$$\mathbf{H}(F_{X_1},F_{X_2}) = -\int_{X_1} U(y;F_{X_1}|x_2,h_1,h_2)dF_{X_1}, \tag{25}$$

where

$$U(y;F_{X_1}|x_2,h_1,h_2) = \int_{X_2}\int_{H_1}\int_{H_2}\sum_{y\in Y} p(y\,|\,x_1,x_2,h_1,h_2)\log p(y\,|\,x_1,x_2,h_1,h_2)dF_{X_2}dF_{H_1}dF_{H_2}. \tag{26}$$

Then, the KTC in **Eq. 23** can be re-written as:

$$-U(y;F_{X_1}|x_2,h_1,h_2) + \mu_1\left(|x_1|^2 - P_1\right) \geq \mathbf{H}\left(F^*_{X_1},F_{X_2}\right) \quad \forall F_{X_1}, \tag{27}$$

with the equality being achieved for any mass point $x_1 \in E^*_{X_1}$, where $E^*_{X_1}$ is the set of point of increase of the optimal $F^*_{X_1}$. Before further examining this KTC, we have the following proposition regarding the log-convexity of the sum of Q functions.

Proposition 2. $\log\left(\sum_{i=1}^M \varepsilon_i\left[Q\left(a_i + b_i\sqrt{x}\right)\right]^2\right)$ is a convex function for non-negative a_i, b_i and for $x \geq 0$.

Proof. The proof is straightforward. Specifically, it can be verified that $\log([Q(a_i + b_i\sqrt{x})]^2)$ is convex. Equivalently, $\epsilon_i Q(a_i + b_i\sqrt{x})^2$ is log-convex. Furthermore, the sum of log-convex functions are log-convex. Therefore, $\sum_{i=1}^M \varepsilon_i[Q(a_i + b_i\sqrt{x})]^2$ is log-convex.

The result in Proposition 2 helps establish the finiteness $U(y;F_{X_1}|x_2,h_1,h_2)$ in **Eq. 27**, which is stated as follows:

Lemma 1. For any F_{X_1} in Ω_1, $U(y;F_{X_1}|x_2,h_1,h_2)$ is finite.

Proof. Because $0 \leq p(y|x_1, x_2, h_1, h_2) \leq 1$, it is apparent that

$$\begin{aligned} &U(y;F_{X_1}|x_2,h_1,h_2) \\ &\leq \int_{X_2}\int_{H_1}\int_{H_2}\left|\sum_{y\in Y} p(y\,|\,x_1,x_2,h_1,h_2)\log p(y\,|\,x_1,x_2,h_1,h_2)\right|dF_{X_2}dF_{H_1}dF_{H_2} \\ &\leq \int_{X_2}\int_{H_1}\int_{H_2}\left|\sum_{y\in Y}\log p(y\,|\,x_1,x_2,h_1,h_2)\right|dF_{X_2}dF_{H_1}dF_{H_2} \\ &\leq \int_{X_2}\int_{H_1}\int_{H_2}\left|4\log\min_{y\in Y} p(y\,|\,x_1,x_2,h_1,h_2)\right|dF_{X_2}dF_{H_1}dF_{H_2}. \end{aligned} \tag{28}$$

As shown in **Appendix B**, we have:

$$\min_{y\in Y} p(y\,|\,x_1,x_2,h_1,h_2) \geq \sum_{i=1}^M \varepsilon_i\left[Q\left(\frac{\sqrt{2}\left(|h_1|\sqrt{|x_1|^2} + |h_2|\sqrt{|x_2|^2}\right)}{\sigma_i}\right)\right]^2. \tag{29}$$

Then, by applying the convexity property of $\log\left(\sum_{i=1}^M \varepsilon_i[Q(a_i + b_i\sqrt{x})]^2\right)$, it follows that:

$$\begin{aligned} &U(y;F_{X_1}|x_2,h_1,h_2) \\ &\leq \int_{X_2}\int_{H_1}\int_{H_2} -4\log\sum_{i=1}^M \varepsilon_i\left[Q\left(\frac{\sqrt{2}\left(|h_1|\sqrt{P_1} + |h_2|\sqrt{|x_2|^2}\right)}{\sigma_i}\right)\right]^2 dF_{X_2}dF_{H_1}dF_{H_2} \\ &\leq -4\log\sum_{i=1}^M \varepsilon_i\left[Q\left(\frac{\sqrt{2}\left(\gamma_1\sqrt{P_1} + \gamma_2\sqrt{P_2}\right)}{\sigma_i}\right)\right]^2 < \infty. \end{aligned} \tag{30}$$

The finiteness of $U(y;F_{X_1}|x_2,h_1,h_2)$ in **Eq. 27** leads to the following important result:

Theorem 1. The optimal input distribution $F^*_{X_1}$ in (22) for a given F_{X_2} has a bounded amplitude.

Proof. The proof is done by contradiction. Specifically, assume that the amplitude of $F^*_{X_1}$ is not bounded. It means there exists a mass point of $F^*_{X_1}$ that goes to infinity. When it happens, it is clear that the LHS of the KTC in 27 goes to infinity for a positive μ_1. On the other hand, the RHS of 27 is the conditional entropy, and it is always less than or equal to 2. That results in a contradiction. Hence, the amplitude of $F^*_{X_1}$ must be bounded.

Given Theorem 1, we can now focus on the set of bounded F_{X_1}, denoted as $F^b_{X_1}$, and consider the following conditional entropy minimization problem for a fixed $F^b_{X_1}$:

$$F^*_{X_2} = \arg \min_{F_{X_2}, E\left[|x_2|^2\right] \le P_2} \mathbf{H}\left(F^b_{X_1}, F_{X_2}\right). \tag{31}$$

A similar result as in Theorem 1 but for $F^*_{X_2}$ is then given in the next theorem.

Theorem 2. The optimal input distribution $F^*_{X_2}$ in **Eq. 31** for a given $F^b_{X_1}$ has a bounded amplitude.

Proof. The proof follows a similar procedure as before, and it can be summarized as follows. We can first establish the KTC for **Eq. 31** as

$$-U\left(y; F_{X_2}|F^b_{X_1}, h_1, h_2\right) + \mu_2\left(|x_2|^2 - P_2\right) \ge \mathbf{H}\left(F^*_{X_2}\right), \tag{32}$$

where μ_2 is the non-negative Lagrangian multiplier. It can then be verified that full-power power P_2 is used, and $\mu_2 > 0$. Furthermore, we have:

$$\begin{aligned} &U(y; F_{X_2}|x_1, h_1, h_2) \\ &= \int_{X_1}\int_{H_1}\int_{H_2}\sum_{y\in Y} p(y \mid x_1, x_2, h_1, h_2)\log p(y \mid x_1, x_2, h_1, h_2) dF^b_{X_1} dF_{H_1} dF_{H_2}. \end{aligned} \tag{33}$$

In a similar manner as in the proof of Lemma 1, we can then show that $U(y; F^*_{X_2}|x_1, h_1, h_2)$ is finite. As a result, if the amplitude of $F^*_{X_2}$ is not bounded, the LHS of **Eq. 32** goes to infinity when $|x_2|$ approaches infinity, while the RHS of **(32)** is finite, which is not possible.

Now, by combining the results from Theorems 1 and 2, we can conclude the capacity-achieving input distributions $F^{**}_{X_1}$ and $F^{**}_{X_2}$ in **Eq. 21** are $\pi/2$ circularly symmetric, and they both have bounded amplitudes. In the following, using a similar analysis as in Winkler (1988); Vu et al. (2019); Ranjbar et al. (2020), we shall demonstrate that both $F^{**}_{X_1}$ and $F^{**}_{X_2}$ in fact have constant amplitudes. First, let $\mathcal{L}_j, j = 1, 2$ is the set of amplitudes of all the distributions that are $\pi/2$ circularly symmetric and bounded amplitude on the feasible set Ω. It then follows that

$$F^{**}_{X_1}, F^{**}_{X_2} = \arg \min_{F_{X_j}\in\mathcal{L}_j, j=1,2} \mathbf{H}(F_{X_1}, F_{X_2}) \tag{34}$$

Since all input distributions are $\pi/2$ circularly symmetric, as similar to the analysis we made earlier, the objective function $\mathbf{H}(F_{X_1}, F_{X_2})$ is independent of the phase $(\theta_{X_1}, \theta_{X_2})$. Equivalently, $\mathbf{H}(F_{X_1}, F_{X_2})$ depends only on the amplitude of the input distributions. More importantly, for a fixed input distribution of one user, the objective function $\mathbf{H}(F_{X_1}, F_{X_2})$ is linear and continuous over the input distribution of the other user. Therefore, for a fixed input distribution of one user, $\mathbf{H}(F_{X_1}, F_{X_2})$ is minimized at an extreme point on the feasible set of the distributions of the other user. As a result, this optimal input must have a single mass point only. The proof of such uniqueness of the extreme point follows the same argument using a convex combination of multiple extreme points we made in the proof of Proposition 1. The detailed proof is therefore omitted here for brevity. By applying the same argument to both user 1 and user 2, it can then be concluded that the optimal $F^{**}_{X_1}$ and $F^{**}_{X_2}$ contain only a single mass point in their amplitudes.

Given the above results, we can conclude that the optimal distributions $F^{**}_{X_1}$ and $F^{**}_{X_2}$ are $\pi/2$ circularly symmetric, and they have constant amplitudes $\sqrt{P_1}$ and $\sqrt{P_2}$, respectively. Then by setting $\phi_{X_1} = \phi_{X_2} = 0$ without changing the value of the conditional entropy as in **Eq. 19**, the sum-capacity of the considered GM MAC is calculated as:

$$\begin{aligned} C_s = 2 - E_{H_1}E_{H_2}\Bigg[\xi\Bigg(\sum_{i=1}^{M}\varepsilon_i Q\Bigg(-\frac{\sqrt{2}\left(|h_1|\sqrt{P_1}\cos(\theta_{h_1}) + |h_2|\sqrt{P_2}\cos(\theta_{h_2})\right)\Re(y)}{\sigma_i}\Bigg) \\ \times Q\Bigg(-\frac{\sqrt{2}\left(|h_1|\sqrt{P_1}\sin(\theta_{h_1}) + |h_2|\sqrt{P_2}\sin(\theta_{h_2})\right)\Im(y)}{\sigma_i}\Bigg)\Bigg)\Bigg]. \end{aligned} \tag{35}$$

Note that $\xi(\cdot)$ is an entropy function of the corresponding distribution.

It is not hard to verify that in the case of a single-user channel under power constraint P and fading H, the single-user capacity C can be obtained from C_s in 35 by setting $P_1 = P$ and $P_2 = 0$, and it is given as:

$$\begin{aligned} C = 2 - E_H\Bigg[\xi\Bigg(\sum_{i=1}^{M}\varepsilon_i Q\Bigg(-\frac{\sqrt{2}\left(|h|\sqrt{P}\cos(\theta_h)\right)\Re(y)}{\sigma_i}\Bigg) \\ Q\Bigg(-\frac{\sqrt{2}\left(|h|\sqrt{P}\sin(\theta_h)\right)\Im(y)}{\sigma_i}\Bigg)\Bigg)\Bigg]. \end{aligned} \tag{36}$$

Furthermore, C can be achieved by a $\pi/2$ circularly symmetric input having a constant input, e.g., QPSK.

As the final note, we would like to mention that the developed results above apply directly to the traditional Gaussian channel. It is because GM include Gaussian as a special case with M = 1.

4 SUM-RATE AND SUM-CAPACITY: NUMERICAL EXAMPLES

In the following, we will provide several examples to verify the optimality of $F^{**}_{X_1}$ and $F^{**}_{X_2}$ in terms of the sum-rate. Unless otherwise stated, we assume that the fading gains have unit variance.

First, let consider a 1-bit ADC MAC under a 2-term GM noise with $\varepsilon_1 = 0.45$, $\varepsilon_2 = 0.55$ and $\sigma_1^2 = 2.1$, $\sigma_2^2 = 0.1$. For this channel, it is assumed that the two users have equal transmit power $P = P_1 = P_2$. We consider several signaling schemes, including phase Shift Keying (PSK) and Quadrature Amplitude Modulation (QAM), for user 1 and user 2, respectively: 1) QPSK + QPSK; 2) QPSK+8-PSK; 3) 16-QAM+16-QAM; and 4) Gaussian + Gaussian. **Figure 3** shows the sum-rates achieved by these modulation schemes over a wide range of SNR, which is defined as SNR = $P/E[|N|]^2$. These sum-rates are numerically calculated from **Eqs. 7, 8, 11** using the corresponding input signals. The sum-capacity calculated from **Eq. 35** is

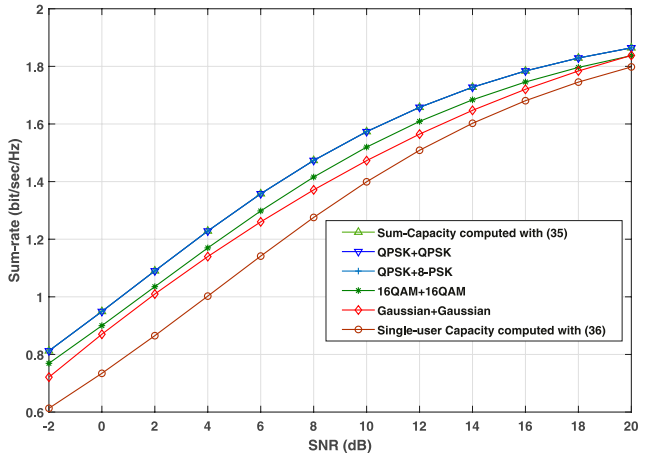

FIGURE 3 | Sum-rates achieved by different pairs of input signals and Single-user capacity over the 2-term GM MAC. The two users are assumed to have equal transmit power P = P_1= P_2 and single-user has transmit power P.

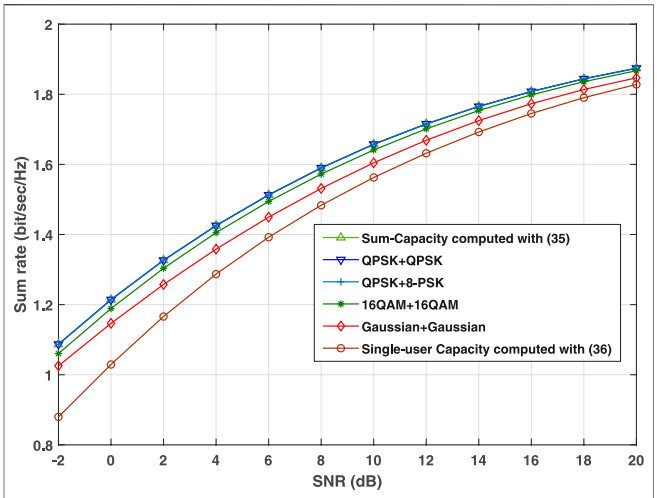

FIGURE 4 | Sum-rates achieved by different pairs of input signals and Single-user capacity over the 3-term GM MAC. The two users are assumed to have equal transmit power P = P_1= P_2 and single-user has transmit power P.

also provided. In addition, the single-user capacity C in **Eq. 36** is plotted as a reference.

The superiority of QPSK + QPSK and QPSK+8-PSK can clearly be seen from **Figure 3**. The reason for that is because such input signals are $\pi/2$ circularly symmetric with constant amplitudes, which are sum-capacity-achieving. It is also clear from **Figure 3** that over the considered SNR range, the single user capacity C is always smaller than the sum-capacity C_s. While the single-user case corresponds to a corner point of the 2-user capacity-region, operating at this corner point is clearly sub-optimal. However, the results shown in **Figure 3** indicates that both C_s and C asymptotically approach 2 bits/sec/Hz at a sufficiently high SNR. This fact can also be verified from **Eqs. 35, 36**.

Our results on the optimal signaling schemes also hold for a general GM channel having any number of Gaussian components. To demonstrate it, **Figure 4** presents the sum-rates achieved by the same signaling schemes over a MAC under GM noise having three Gaussian components with ε_1 = 0.9, ε_2 = 0.05, ε_3 = 0.05 and $\sigma_1^2 = 0.2, \sigma_2^2 = 0.1, \sigma_3^2 = 16.3$. Note that both users are assumed to use the same transmit power. As we mentioned earlier, the sum-capacity is calculated using **Eq. 35**, while the other sum-rates are obtained from **Eqs. 7, 8, 11**. For comparison, the single-user capacity in **Eq. 36** is also provided. It can be seen from **Figure 4** that QPSK + QPSK and QPSK+8-PSK outperform the other signaling schemes in terms of the sum-rate. As similar to the previous results for the 2-term GM channel, the sum-capacity C_s is significantly larger than the single-user capacity C over the SNR range of interest.

In **Figures 5**, **6**, the sum-rates are plotted for the considered 2-GM and 3-GM channels, respectively, but using un-equal transmit power with P_1 = P and P_2 = 3P. Note that in this case, we still define SNR as SNR = $P/E[|N|]^2$. Clearly, the optimality of QPSK + QPSK and QPSK+8-PSK is persistent

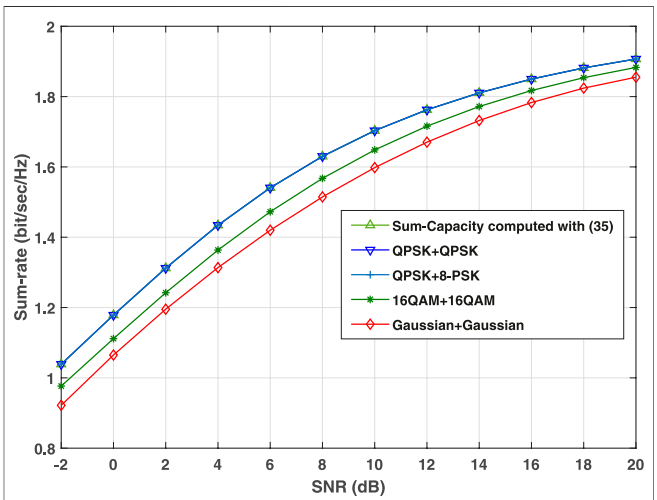

FIGURE 5 | Sum-rates achieved by different pairs of input signals over the 2-term GM MAC. The two users are assumed to have unequal transmit power P_1 = P and P_2 = 3P.

with the results achieved in the case of equal transmit power. Note that we also observe the same sub-optimality of a single-user capacity case in terms of sum-capacity. The results, however, are omitted for brevity.

Finally, **Figure 7** compares the sum-capacities of three different channels: the Gaussian, 2-term GM, and 3-term GM channels. Note that we use the same 2-term and 3-term GMs as before. For simplicity, we assume the equal transmit power again with P_1 = P and P_2 = P, and use SNR = $P/E[|N|]^2$ as before. With the chosen parameters, we achieve the highest sum-capacity over the 3-term GM channel. The Gaussian noise is the worst-case noise in this case. However, it is clear from **Eq. 35** that the sum

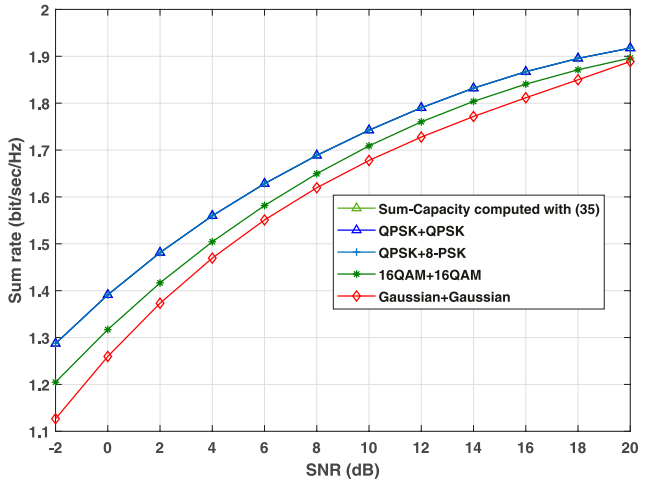

FIGURE 6 | Sum-rates achieved by different pairs of input signals over the 3-term GM MAC. The two users are assumed to have unequal transmit power $P_1 = P$ and $P_2 = 3P$.

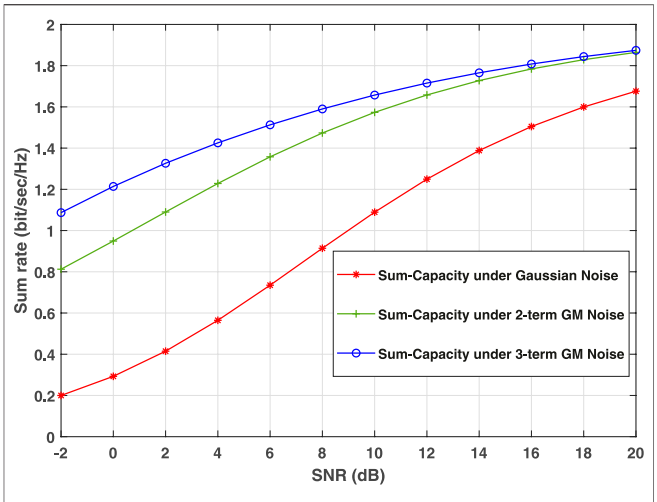

FIGURE 7 | Sum-capacities of MACs under different types of noise: Gaussian, 2-term GM, and 3-term GM.

capacity C_s is sensitive to the choice of M and the set of $\{\epsilon_i\}$ and $\{\sigma_i\}$, $1 \le i \le M$. Due to the complexity of the function C_s in **Eq. 35**, it is not straightforward to analytically compare the sum-capacities of different Gaussian and GM channels. We believe that such interesting investigation requires additional studies.

5 CONCLUSION

In this paper, we have addressed the optimal input distributions and the sum-capacity of a 2-user Rayleigh fading MAC under a general Gaussian-mixture noise plus interference with 1-bit ADC. The phases of the optimal inputs were first shown to be $\pi/2$ circularly symmetric. By exploiting this result, it was proved that the amplitudes of the optimal input distributions must only have a single mass point in order to minimize the conditional entropy. As a result, the sum-capacity achieving signaling schemes are $\pi/2$ circularly symmetric with a single mass point amplitude using full power. The advantages of the proposed signaling schemes in terms of the sum-rate were also clearly demonstrated.

DATA AVAILABILITY STATEMENT

The raw data supporting the conclusions of this article will be made available by the authors, without undue reservation.

AUTHOR CONTRIBUTIONS

All authors listed have made a substantial, direct, and intellectual contribution to the work and approved it for publication.

FUNDING

This work was partially supported by Air Force Research Lab/ Intelligent Fusion Technology under SBIR Grant No. IFT079-02.

REFERENCES

Abou-Faycal, I. C., Trott, M. D., and Shamai, S. (2001). The Capacity of Discrete-Time Memoryless Rayleigh-Fading Channels. *IEEE Trans. Inform. Theor.* 47, 1290–1301. doi:10.1109/18.923716

Bayram, S., and Gezici, S. (2010). On the Performance of Single-Threshold Detectors for Binary Communications in the Presence of Gaussian Mixture Noise. *IEEE Trans. Commun.* 58, 3047–3053. doi:10.1109/tcomm.2010.091710.090124

Bhatia, V., and Mulgrew, B. (2007). Non-parametric Likelihood Based Channel Estimator for Gaussian Mixture Noise. *Signal. Process.* 87, 2569–2586. doi:10.1016/j.sigpro.2007.04.006

Borwein, J., and Lewis, A. S. (2010). *Convex Analysis and Nonlinear Optimization: Theory and Examples*. Springer Science & Business Media.

Cao, J., Hranilovic, S., and Chen, J. (2014). Capacity-Achieving Distributions for the Discrete-Time Poisson Channel-Part I: General Properties and Numerical Techniques. *IEEE Trans. Commun.* 62, 194–202. doi:10.1109/tcomm.2013.112513.130142

Choi, J., Lee, G., Alkhateeb, A., Gatherer, N., and Evans, B. L. (2020). Advanced Receiver Architectures for Millimeter-Wave Communications with Low-Resolution ADCs. *IEEE Commun. Mag.* 58, 42–48. doi:10.1109/MCOM.001.2000122

Cover, T. M., and Thomas, J. A. (2006). *Elements of Information Theory*. 2nd edition. Wiley-Interscience.

Das, A. (2000). "Capacity-achieving Distributions for Non-gaussian Additive Noise," in 2017 IEEE International Symposium on Information Theory (ISIT), Sorrento, Italy, June, 2000.

Dytso, A., Bustin, R., Poor, H. V., and Shitz, S. S. (2017). "On Additive Channels with Generalized Gaussian Noise," in 2017 IEEE International Symposium on Information Theory (ISIT), Aachen, Germany, June 25–30, 2017, 426–430. doi:10.1109/isit.2017.8006563

ElSawy, H., Hossain, E., and Haenggi, M. (2013). Stochastic Geometry for Modeling, Analysis, and Design of Multi-Tier and Cognitive Cellular Wireless Networks: A Survey. *IEEE Commun. Surv. Tutorials* 15, 996–1019. doi:10.1109/surv.2013.052213.00000

Erseghe, T., Cellini, V., and Donà, G. (2008). On UWB Impulse Radio Receivers Derived by Modeling MAI as a Gaussian Mixture Process. *IEEE Trans. Wireless Commun.* 7, 2388–2396. doi:10.1109/twc.2008.070133

Fahs, J., Ajeeb, N., and Abou-Faycal, I. (2012). "The Capacity of Average Power Constrained Additive Non-gaussian Noise Channels," in International Conference on Telecommunications (ICT), Jounieh, Lebanon, April 23–25, 2012. doi:10.1109/ictel.2012.6221320

FCC (2020). 3.5 GHz Band Overview. Available at: https://www.fcc.gov/35-ghz-band-overview.

Feng, D., Lu, L., Yuan-Wu, Y., Li, G., Li, S., and Feng, G. (2014). Device-to-device Communications in Cellular Networks. *IEEE Commun. Mag.* 52, 49–55. doi:10.1109/mcom.2014.6807946

Fodor, G., Dahlman, E., Mildh, G., Parkvall, S., Reider, N., Miklós, G., et al. (2012). Design Aspects of Network Assisted Device-To-Device Communications. *IEEE Commun. Mag.* 50, 170–177. doi:10.1109/mcom.2012.6163598

Gamal, A., and Kim, Y. (2011). *Network Information Theory*. Cambridge University Press.

Gulati, K., Evans, B. L., Andrews, J. G., and Tinsley, K. R. (2010). Statistics of Co-channel Interference in a Field of Poisson and Poisson-Poisson Clustered Interferers. *IEEE Trans. Signal. Process.* 58, 6207–6222. doi:10.1109/tsp.2010.2072922

Irio, L., Oliveira, R., da Costa, D. B., and Alouini, M.-S. (2020). Impact of Wireless-Powered Communications in Coexisting mobile Networks. *IEEE Wireless Commun. Lett.* 9, 1. doi:10.1109/LWC.2020.2980524

Irio, L., Oliveira, R., and da Costa, D. B. (2019). Highly Accurate Approaches for the Interference Modeling in Coexisting Wireless Networks. *IEEE Commun. Lett.* 23, 1652–1656. doi:10.1109/LCOMM.2019.2924887

Jacobsson, S., Durisi, G., Coldrey, M., Gustavsson, U., and Studer, C. (2017). Throughput Analysis of Massive MIMO Uplink with Low-Resolution ADCs. *IEEE Trans. Wireless Commun.* 16, 4038–4051. doi:10.1109/TWC.2017.2691318

Jeon, Y.-S., Do, H., Hong, S.-N., and Lee, N. (2019). Soft-output Detection Methods for Sparse Millimeter-Wave MIMO Systems with Low-Precision ADCs. *IEEE Trans. Commun.* 67, 2822–2836. doi:10.1109/tcomm.2019.2892048

Kenarsari-Anhari, A., and Lampe, L. (2010). Performance Analysis for BICM Transmission over Gaussian Mixture Noise Fading Channels. *IEEE Trans. Commun.* 58, 1962–1972. doi:10.1109/TCOMM.2010.07.090337

Krone, S., and Fettweis, G. (2010). "Fading Channels with 1-bit Output Quantization: Optimal Modulation, Ergodic Capacity and Outage Probability," in 2010 IEEE Information Theory Workshop, Cairo, Egypt, January 6–8, 2010 (IEEE), 1–5. doi:10.1109/cig.2010.5592653

Le, D.-A., Vu, H. V., Tran, N. H., Gursoy, M. C., and Le-Ngoc, T. (2016). Approximation of Achievable Rates in Additive Gaussian Mixture Noise Channels. *IEEE Trans. Commun.* 64, 5011–5024. doi:10.1109/TCOMM.2016.2602342

Lin, X., Andrews, J., Ghosh, A., and Ratasuk, R. (2014). An Overview of 3GPP Device-To-Device Proximity Services. *IEEE Commun. Mag.* 52, 40–48. doi:10.1109/mcom.2014.6807945

Liu, T., Tong, J., Guo, Q., Xi, J., Yu, Y., and Xiao, Z. (2019). Energy Efficiency of Massive MIMO Systems with Low-Resolution ADCs and Successive Interference Cancellation. *IEEE Trans. Wireless Commun.* 18, 3987–4002. doi:10.1109/twc.2019.2920129

Mezghani, A., and Nossek, J. A. (2008). "Analysis of Rayleigh-Fading Channels with 1-bit Quantized Output," in 2008 IEEE International Symposium on Information Theory (IEEE), Toronto, Canada, July 7–12, 2008, 260–264. doi:10.1109/isit.2008.4594988

Middleton, D. (1999). Non-Gaussian Noise Models in Signal Processing for Telecommunications: New Methods an Results for Class A and Class B Noise Models. *IEEE Trans. Inform. Theor.* 45, 1129–1149. doi:10.1109/18.761256

Mo, J., Alkhateeb, A., Abu-Surra, S., and Heath, R. W. (2017). Hybrid Architectures with Few-Bit ADC Receivers: Achievable Rates and Energy-Rate Tradeoffs. *IEEE Trans. Wireless Commun.* 16, 2274–2287. doi:10.1109/TWC.2017.2661749

Mo, J., and Heath, R. W. (2015). Capacity Analysis of One-Bit Quantized MIMO Systems with Transmitter Channel State Information. *IEEE Trans. Signal. Process.* 63, 5498–5512. doi:10.1109/tsp.2015.2455527

Moghimi, F., Nasri, A., and Schober, R. (2011). Adaptive L_p-Norm Spectrum Sensing for Cognitive Radio Networks. *IEEE Trans. Commun.* 59, 1934–1945. doi:10.1109/tcomm.2011.051311.090588

Mollen, C., Choi, J., Larsson, E. G., and Heath, R. W. (2017). Uplink Performance of Wideband Massive MIMO with One-Bit ADCs. *IEEE Trans. Wireless Commun.* 16, 87–100. doi:10.1109/TWC.2016.2619343

Nasri, A., and Schober, R. (2009). Performance of BICM-SC and BICM-OFDM Systems with Diversity Reception in Non-gaussian Noise and Interference. *IEEE Trans. Commun.* 57, 3316–3327. doi:10.1109/tcomm.2009.11.080180

Oettli, W. (1974). Capacity-achieving Input Distributions for Some Amplitude-Limited Channels with Additive Noise (corresp.). *IEEE Trans. Inform. Theor.* 20, 372–374. doi:10.1109/TIT.1974.1055225

Osseiran, A., Boccardi, F., Braun, V., Kusume, K., Marsch, P., Maternia, M., et al. (2014). Scenarios for 5G mobile and Wireless Communications: The Vision of the METIS Project. *IEEE Commun. Mag.* 52, 26–35. doi:10.1109/mcom.2014.6815890

Quek, T. Q. S., de la Roche, G., Güvenç, I., and Kountouris, M. (2013). *Small Cell Networks: Deployment, PHY Techniques, and Resource Management*. 1st edn. Cambridge University Press.

Rahman, M. H., Ranjbar, M., Tran, N. H., and Pham, K. (2020b). "Capacity-achieving Signal and Capacity of Gaussian Mixture Channels with 1-bit Output Quantization," in ICC 2020 - 2020 IEEE International Conference on Communications (ICC), Virtual Conference, Jun 7–11, 2020, 1–6. doi:10.1109/ICC40277.2020.9149428

Rahman, M., Ranjbar, M., and Tran, N. (2020a). On the Capacity-Achieving Scheme and Capacity of 1-bit Adc Gaussian-Mixture Channels. *EAI Endorsed Trans. Ind. Networks Intell. Syst.* 7, 162830. doi:10.4108/eai.31-1-2020.162830

Ranjbar, M., Tran, N. H., Nguyen, T. V., Gursoy, M. C., and Nguyen-Le, H. (2018). Capacity-achieving Signals for point-to-point and Multiple-Access Channels under Non-gaussian Noise and Peak Power Constraint. *IEEE Access* 6, 30977–30989. doi:10.1109/access.2018.2837056

Ranjbar, M., Tran, N. H., Vu, M. N., Nguyen, T. V., and Cenk Gursoy, M. (2020). Capacity Region and Capacity-Achieving Signaling Schemes for 1-bit ADC Multiple Access Channels in Rayleigh Fading. *IEEE Trans. Wireless Commun.* 19, 6162–6178. doi:10.1109/twc.2020.3000610

Ranjbar, M., Vu, M., Tran, N., Pham, K., and Nguyen, D. (2019). "On the Sum-Capacity-Achieving Distributions and Sum-Capacity of 1-bit Adc Macs in Rayleigh Fading," in ICC 2019-2019 IEEE International Conference on Communications (ICC), Shanghai, China, May 20–24, 2019 (IEEE), 1–6. doi:10.1109/icc.2019.8761097

Rassouli, B., Varasteh, M., and Gündüz, D. (2018). Gaussian Multiple Access Channels with One-Bit Quantizer at the Receiver. *Entropy* 20, 686. doi:10.3390/e20090686

Reynolds, D. A. (2009). *Gaussian Mixture Models*. [Dataset]. MIT Lincoln Laboratory.

Chen, S., and Zhao, J. (2014). The Requirements, Challenges, and Technologies for 5G of Terrestrial mobile Telecommunication. *IEEE Commun. Mag.* 52, 36–43. doi:10.1109/mcom.2014.6815891

Singh, J., Dabeer, O., and Madhow, U. (2009). On the Limits of Communication with Low-Precision Analog-To-Digital Conversion at the Receiver. *IEEE Trans. Commun.* 57, 3629–3639. doi:10.1109/TCOMM.2009.12.080559

Stein, D. W. J. (1995). Detection of Random Signals in Gaussian Mixture Noise. *IEEE Trans. Inform. Theor.* 41, 1788–1801. doi:10.1109/18.476307

Studer, C., and Durisi, G. (2016). Quantized Massive MU-MIMO-OFDM Uplink. *IEEE Trans. Commun.* 64, 2387–2399. doi:10.1109/TCOMM.2016.2558151

Tchamkerten, A. (2004). On the Discreteness of Capacity-Achieving Distributions. *IEEE Trans. Inform. Theor.* 50, 2773–2778. doi:10.1109/tit.2004.836662

Vu, H. V., Tran, N. H., Gursoy, M. C., Le-Ngoc, T., and Hariharan, S. I. (2015). Capacity-achieving Input Distributions of Additive Quadrature Gaussian Mixture Noise Channels. *IEEE Trans. Commun.* 63, 3607–3620. doi:10.1109/tcomm.2015.2451096

Vu, M. N., Tran, N. H., Wijeratne, D. G., Pham, K., Lee, K.-S., and Nguyen, D. H. N. (2019). Optimal Signaling Schemes and Capacity of Non-coherent Rician Fading Channels with Low-Resolution Output

Quantization. *IEEE Trans. Wireless Commun.* 18, 2989–3004. doi:10.1109/twc.2019.2907952

Vu, M., Wijeratne, D., Tran, N., and Pham, K. (2018). "Optimal Signaling Scheme and Capacity of Non-coherent Rician Fading Channels with 1-bit Output Quantization," in 2018 IEEE International Conference on Communications (ICC), Kansas City, MO, May 20–24, 2018 (IEEE), 1–6. doi:10.1109/icc.2018.8422260

Winkler, G. (1988). Extreme Points of Moment Sets. *Mathematics OR* 13, 581–587. doi:10.1287/moor.13.4.581

Xiaodong Wang, X., and Poor, H. V. (1999). Robust Multiuser Detection in Non-gaussian Channels. *IEEE Trans. Signal. Process.* 47, 289–305. doi:10.1109/78.740103

Xiong, Y., Wei, N., Zhang, Z., Li, B., and Chen, Y. (2017). Channel Estimation and IQ Imbalance Compensation for Uplink Massive MIMO Systems with Low-Resolution ADCs. *IEEE Access* 5, 6372–6388. doi:10.1109/ACCESS.2017.2690439

Xu, J., Xu, W., Zhang, H., Li, G. Y., and You, X. (2018). Performance Analysis of Multi-Cell Millimeter Wave Massive MIMO Networks with Low-Precision ADCs. *IEEE Trans. Commun.* 67, 302–317. doi:10.1109/TCOMM.2018.2874963

Zhang, J., Dai, L., Sun, S., and Wang, Z. (2016). On the Spectral Efficiency of Massive MIMO Systems with Low-Resolution ADCs. *IEEE Commun. Lett.* 20, 842–845. doi:10.1109/LCOMM.2016.2535132

Conflict of Interest: The authors declare that the research was conducted in the absence of any commercial or financial relationships that could be construed as a potential conflict of interest.

Publisher's Note: All claims expressed in this article are solely those of the authors and do not necessarily represent those of their affiliated organizations, or those of the publisher, the editors and the reviewers. Any product that may be evaluated in this article, or claim that may be made by its manufacturer, is not guaranteed or endorsed by the publisher.

APPENDIX A

Proof that $\mathbf{H}(Y; F_{X_1}^{\pi/2}, F_{X_2}^{\pi/2} \mid H_1, H_2) = 2$

From **Eq. 13**, it can be verified that $p(y|x_1, x_2, h_1, h_2) = p(ye^{-j\frac{k\pi}{2}}|x_1 e^{j\frac{k\pi}{2}}, x_2 e^{j\frac{k\pi}{2}}, h_1, h_2)$. Then we have the following:

$$\begin{aligned}
&p\left(y; F_{X_1}^{\pi/2}, F_{X_2}^{\pi/2}|h_1, h_2\right)\\
&= \frac{1}{16}\sum_{k=0}^{3}\sum_{l=0}^{3}\int_{X_1}\int_{X_2} p(y \mid x_1, x_2, h_1, h_2) dF_{X_1}\left(x_1 e^{j\frac{k\pi}{2}}\right) dF_{X_2}\left(x_2 e^{j\frac{l\pi}{2}}\right)\\
&= \frac{1}{16}\sum_{k=0}^{3}\sum_{l=0}^{3}\int_{X_1}\int_{X_2} p(y \mid x_1, x_2, h_1, h_2) dF_{X_1}\left(x_1 e^{j\frac{k\pi}{2}}\right) dF_{X_2}\left(x_2 e^{j((k+l) \bmod 4)\frac{\pi}{2}}\right)\\
&= \frac{1}{16}\sum_{k=0}^{3}\sum_{l=0}^{3}\int_{X_1}\int_{X_2} p\left(y \mid x_1 e^{j\frac{k\pi}{2}}, x_2 e^{j((k+l) \bmod 4)\frac{\pi}{2}}, h_1, h_2\right) dF_{X_1} dF_{X_2}\\
&= \frac{1}{16}\sum_{l=0}^{3}\int_{X_1}\int_{X_2}\sum_{k=0}^{3} p\left(ye^{j\frac{k\pi}{2}}|x_1, x_2 e^{-j\frac{l\pi}{2}}, h_1, h_2\right) dF_{X_1} dF_{X_2}\\
&= \frac{1}{16}\times 4 = \frac{1}{4}.
\end{aligned} \tag{37}$$

The third equality is based on the variable transformation and the fourth equality is due to the fact that $p(ye^{-j\frac{k\pi}{2}} \mid x_1 e^{j\frac{k\pi}{2}}, x_2 e^{j\frac{k\pi}{2}}, h_1, h_2) = p(ye^{j\frac{k\pi}{2}} \mid x_1 e^{-j\frac{k\pi}{2}}, x_2 e^{-j\frac{k\pi}{2}}, h_1, h_2)$. Thus, the output is uniform, and $\mathbf{H}(Y; F_{X_1}^{\pi/2}, F_{X_2}^{\pi/2} \mid H_1, H_2) = 2$.

APPENDIX B

The Inequality $\underset{Y\in\mathcal{Y}}{\mathrm{MIN}} P(Y \mid X_1, X_2, H_1, H_2) \geq \sum_{i=1}^{M} \varepsilon_i \left[Q\left(\frac{\sqrt{2}\left(|H_1|\sqrt{|X_1|^2}+|H_2|\sqrt{|X_2|^2}\right)}{\sigma_i} \right) \right]^2$.

We Have

$$\begin{aligned}
&p(y \mid x_1, x_2, h_1, h_2)\\
&= \sum_{i=1}^{M} \varepsilon_i Q\left(-\frac{\sqrt{2}\,\Re(h_1 x_1 + h_2 x_2)}{\sigma_i}\Re(y)\right) Q\left(-\frac{\sqrt{2}\,\Im(h_1 x_1 + h_2 x_2)}{\sigma_i}\Im(y)\right)\\
&\geq \sum_{i=1}^{M} \varepsilon_i Q\left(\left|\frac{\sqrt{2}\,\Re(h_1 x_1 + h_2 x_2)}{\sigma_i}\right|\right) Q\left(\left|\frac{\sqrt{2}\,\Im(h_1 x_1 + h_2 x_2)}{\sigma_i}\right|\right)\\
&\geq \sum_{i=1}^{M} \varepsilon_i Q\left(\frac{\sqrt{2}\,(|h_1\|x_1| + |h_2\|x_2|)}{\sigma_i}\right) Q\left(\frac{\sqrt{2}\,(|h_1\|x_1| + |h_2\|x_2|)}{\sigma_i}\right)\\
&= \sum_{i=1}^{M} \varepsilon_i \left[Q\left(\frac{\sqrt{2}\left(|h_1|\sqrt{|x_1|^2} + |h_2|\sqrt{|x_2|^2}\right)}{\sigma_i}\right)\right]^2.
\end{aligned} \tag{38}$$

Note that the last inequality comes from the fact that Q(x) is a decreasing function of a positive x.